Development 134, 2685-2695 (2007) doi:10.1242/dev.008268

Binary cell fate specification during *C. elegans* embryogenesis driven by reiterated reciprocal asymmetry of TCF POP-1 and its coactivator β-catenin SYS-1

Shuyi Huang, Premnath Shetty, Scott M. Robertson and Rueyling Lin*

C. elegans embryos exhibit an invariant lineage comprised primarily of a stepwise binary diversification of anterior-posterior (A-P) blastomere identities. This binary cell fate specification requires input from both the Wnt and MAP kinase signaling pathways. The nuclear level of the TCF protein POP-1 is lowered in all posterior cells. We show here that the β-catenin SYS-1 also exhibits reiterated asymmetry throughout multiple A-P divisions and that this asymmetry is reciprocal to that of POP-1. Furthermore, we show that SYS-1 functions as a coactivator for POP-1, and that the SYS-1-to-POP-1 ratio appears critical for both the anterior and posterior cell fates. A high ratio drives posterior cell fates, whereas a low ratio drives anterior cell fates. We show that the SYS-1 and POP-1 asymmetries are regulated independently, each by a subset of genes in the Wnt/MAP kinase pathways. We propose that two genetic pathways, one increasing SYS-1 and the other decreasing POP-1 levels, robustly elevate the SYS-1-to-POP-1 ratio in the posterior cell, thereby driving A-P differential cell fates.

KEY WORDS: *C. elegans*, TCF/POP-1, β-catenin/SYS-1, Cell fate specification

INTRODUCTION

In the *C. elegans* embryo, blastomere fates are determined early through a combination of the spatiotemporally controlled expression of maternally supplied transcription factors and highly specific cell-cell interactions (Kemphues and Strome, 1997; Schnabel and Priess, 1997). After initial fate specification, each blastomere generates specific terminally differentiated cell types via an invariant lineage. Lineage analyses using genetic mutants suggest that the *C. elegans* embryo invariant lineage is primarily composed of stepwise bifurcations of blastomere specification at anterior-posterior (A-P) cell divisions (Kaletta et al., 1997).

Mutations in the gene *lit-1*, which encodes a Nemo-like MAP kinase (Meneghini et al., 1999; Rocheleau et al., 1999), suggest that the LIT-1 protein functions in at least six consecutive A-P divisions to effect a binary switch whereby the posterior cell of two equivalent cells assumes the posterior cell fate (Kaletta et al., 1997). The nuclear level of LIT-1 is higher in posterior cells where its activity is required, compared with their anterior sisters (Lo et al., 2004; Takeshita and Sawa, 2005). The A-P asymmetry of LIT-1 levels is reciprocal to that of the *C. elegans* TCF protein, POP-1, which is detected at a higher level in the nuclei of anterior cells of all A-P divisions examined (Lin et al., 1998; Lin et al., 1995). Both LIT-1 and POP-1 A-P asymmetries require the MAP kinase kinase kinase MOM-4, a *C. elegans* β-catenin WRM-1, and a lesser contribution from other components of the Wnt pathway (Lin et al., 1998; Lo et al., 2004; Maduro et al., 2002; Meneghini et al., 1999; Park and Priess, 2003; Rocheleau et al., 1999; Shin et al., 1999; Thorpe et al., 1997). WRM-1 has been shown to bind directly to LIT-1 and activate its kinase activity in vitro (Rocheleau et al., 1999). We have shown previously that specific phosphorylation of POP-1 by LIT-1–WRM-1 promotes its interaction with a 14-3-3 protein, leading to nuclear export (Lo et al., 2004). Therefore, in posterior cells, as compared with their anterior sisters, nuclear levels of LIT-1 are high and those of POP-1 are low.

At the 4-cell stage, a Wnt/MAPK signal from P2 to EMS specifies the posterior daughter of EMS, E, to become an endoderm precursor (Goldstein, 1992). The anterior daughter of EMS, MS, generates mesoderm. Most mutations in either the Wnt or MAP kinase signaling pathways result in a non-fully penetrant transformation of E to MS (the Mom phenotype) (Kaletta et al., 1997; Rocheleau et al., 1997; Thorpe et al., 1997). Mutation in *pop-1* results in MS adopting the fate of E (Lin et al., 1995). We and others have shown that POP-1 both represses E fate in the MS blastomere (Calvo et al., 2001; Lin et al., 1995; Rocheleau et al., 1997; Thorpe et al., 1997) and promotes endoderm formation from E (Maduro et al., 2005b; Shetty et al., 2005). We showed that Wnt/MAPK signaling converts POP-1 from a repressor to an activator of target genes (Shetty et al., 2005). Activation of these target genes in E by POP-1 requires the N-terminal domain of POP-1 and that the POP-1 nuclear level in E be lowered. The requirement for the N-terminal domain of POP-1, similar in sequence to the N-terminal domains of other TCF proteins involved in binding β-catenin (van de Wetering et al., 1997), suggests a β-catenin co-activator.

The *C. elegans* genome encodes four β-catenin-related proteins: HMP-2, BAR-1, WRM-1 and SYS-1. The *hmp-2* mutant phenotype suggests a function exclusively in cell adhesion (Costa et al., 1998) and, although BAR-1 can function as a POP-1 transcriptional coactivator in vitro, a *bar-1* likely null mutation has no observable embryonic defect (Eisenmann et al., 1998). WRM-1 is required for asymmetric cell fates in *C. elegans* embryogenesis (Rocheleau et al., 1997), but it has never been shown to physically interact with POP-1, nor has it been shown to function as a TCF/POP-1 co-activator (Kidd et al., 2005; Korswagen et al., 2000; Natarajan et al., 2001; Rocheleau et al., 1999). SYS-1 is required for asymmetric divisions of the somatic gonad precursors (Kidd et al., 2005; Miskowski et al., 2001), and can function as a POP-1 transcriptional coactivator in vitro, via interaction with the N-terminal β-catenin-binding domain

Department of Molecular Biology, University of Texas Southwestern Medical Center, 6000 Harry Hines Boulevard, Dallas, TX 75390, USA.

*Author for correspondence (e-mail: rueyling.lin@utsouthwestern.edu)

Accepted 15 May 2007

of POP-1 (Kidd et al., 2005). Recently, SYS-1 has been implicated in endoderm precursor specification (Phillips et al., 2007). Whereas animals homozygous for a reduction-of-function mutation are sterile, *sys-1(RNAi)* resulted in a very low penetrance gutless phenotype.

We show here that SYS-1 is a limiting coactivator for POP-1 in the activation of Wnt/MAPK-responsive genes in the E blastomere. SYS-1 exhibits a reiterated asymmetry that is reciprocal to the reiterated asymmetry of nuclear POP-1 through all A-P divisions examined. We show that the SYS-1-to-POP-1 ratio appears critical for both anterior and posterior cell fates at multiple divisions: a high ratio drives the posterior cell fate, whereas a low ratio drives the anterior cell fate. SYS-1 and POP-1 levels are regulated in opposite directions by two pathways known to regulate endoderm specification: SYS-1 levels are increased primarily by the MOM-2/MOM-5/APR-1 pathway, whereas nuclear POP-1 levels are decreased primarily by the MOM-4/LIT-1/WRM-1 pathway. Together, these two pathways efficiently increase the SYS-1-to-POP-1 ratio in the posterior cell, promoting asymmetric cell fates.

MATERIALS AND METHODS

Strains

N2 was used as the wild-type strain. Genetic markers: LGI, *pop-1(zu189)*, *dpy-5(e61)*, *mom-5(or57)*, *mom-4(ne19)*, *sys-1(q544)*, *fog-3(q520)*, *teIs3(P$_{med-1}$gfp::pop-1)*, *hT1(I:V)*, *szT1(I:X)*; LGII, *rol-1(e91)*, *mom-3(or78)*, *mnC1*; LGIII, *unc-119(ed3)*, *lit-1(t1512)*, *lit-1(t1534)*, *unc32(e189)*; LGIV, *teIs46(P$_{end-1}$gfp::H2B)*; LGV, *mom-2(or42)*, *DnT1(IV;V)*, *teIs18(P$_{sdz-23}$gfp::H2B)*; LGX, *mom-1(or10)*, *unc-6(n102)*. TX796 [*teEx321(P$_{med-1}$gfp::sys-1)*]. TX585 [*teIs18(P$_{sdz-23}$gfp::H2B)(V)*]. TX691 [*teIs46(P$_{end-1}$gfp::H2B)(IV)*] (Shetty et al., 2005). TX932 [*sys-1(q544)/fog-3(q470)(I); teIs3(P$_{med-1}$gfp::pop-1)(V)*] (Miskowski et al., 2001). TX964 [*teIs98(P$_{pie-1}$gfp::sys-1)*]. JM139 [*P$_{pho-1}$ NLS::gfp::H2B*] (a gift from J. McGhee and J. Yan, University of Calgary, Alberta, Canada). *teIs98* was generated by microparticle bombardment (Praitis et al., 2001). All other strains were obtained from the *Caenorhabditis* Genetics Center (CGC).

RNA interference (RNAi)

sys-1 RNAi was performed by feeding L3 larvae with RNAi bacteria followed by injection. We obtained 3-4% gutless embryos upon *sys-1(RNAi)* into JK2761 [*sys-1(q544)/unc-29(e1072) fog-3(q470)(I)*] but not wild-type N2. RNAi experiments were performed by injection for *imb-4*, *skn-1*, *med-1/med-2*, *apr-1*, *lit-1* and *mom-5* (Rogers et al., 2002) and by feeding for *wrm-1*, *pop-1*, *skn-1*, *rpn-8*, *pas-4*, *pbs-2*, *ran-3* and *ran-4* (Timmons and Fire, 1998). RNAi by feeding for each of the genes listed here resulted in nearly 100% dead embryos. For *pop-1* mild depletion, *pop-1*-feeding RNAi bacteria were diluted with HT115 bacteria. Embryos laid 16-30 hours after injection or 48-60 hours after feeding were collected and either allowed to differentiate for 12 more hours, a period long enough for wild-type control embryos to hatch, or processed for imaging.

Analysis of embryos and imaging

Expression of Wnt target genes upon *sys-1* depletion was analyzed as described previously (Shetty et al., 2005). Embryos were collected from *mom* mutant or RNAi hermaphrodites, and either assayed for GFP and scored later for gut formation, or fixed for immunofluorescence. *teEx321* was crossed into JM139 hermaphrodites. Embryos were collected and assayed first for GFP::SYS-1 in early embryos, then PHO-1 reporter GFP in the newly hatched larvae.

GFP::SYS-1 was analyzed by imaging of live embryos or by immunofluorescence using anti-GFP (Invitrogen) and anti-POP-1 antibodies (Lin et al., 1998). Images were collected as stacks along the *z*-axis with 3 microns between adjacent images (~16 slices per specimen). 16-bit images were collected with raw pixel values within the linear range of the CCD camera and processed and quantified using ImageJ (Lo et al., 2004; Rogers et al., 2002). Owing to variation in expression levels from embryo to embryo, for embryos with abolished GFP::SYS-1 asymmetry we could not determine whether the level of GFP::SYS-1 was elevated in anterior cells, decreased in posterior cells, or both.

Intestinal cells were identified by their birefringent gut-specific granules under polarized optics and by staining with the monoclonal antibody ICB4 (Kemphues et al., 1988). Pharyngeal tissues were identified based on morphology using DIC and immunofluorescence using the monoclonal antibody 3NB12 (Priess and Thomson, 1987). Pharyngeal staining was imaged as a stack along the *z*-axis to facilitate the counting of pm7 cells.

RESULTS

sys-1 activity is required for the activation of Wnt-responsive genes in the E blastomere

To investigate the potential of β-catenin SYS-1 as a co-activator for POP-1 in the E blastomere, we examined the effect of *sys-1* depletion on the expression of the Wnt-responsive, E-specific genes *sdz-23* and *end-1* (Robertson et al., 2004; Shetty et al., 2005; Zhu et al., 1997). Depletion of *sys-1* by RNAi resulted in a reduction in the expression levels of both *sdz-23* and *end-1* reporter genes in all embryos examined (n>200), similar to that observed when *pop-1* is removed (Fig. 1A,C,E,F; data not shown). However, *sys-1*-depletion did not result in derepression of either E-specific reporter in the MS lineage (Fig. 1A-D), or in defects in GFP::POP-1 asymmetry (data not shown). These results suggest that *sys-1* functions in activation of Wnt target gene expression in E, downstream or independent of the regulation of nuclear POP-1 levels.

sys-1(RNAi) resulted in nearly 100% dead embryos arrested without proper morphogenesis, but nonetheless with differentiated tissue types, such as epidermal, pharyngeal and muscle cells (Fig. 1H). Despite pleiotropic terminal phenotypes, 3-4% of *sys-1(RNAi)* embryos were consistently observed to lack intestine (n=497, Fig. 1I), a percentage of gutless similar to that observed in *pop-1(RNAi)* embryos (Maduro et al., 2005b). The maternal transcription factor SKN-1 functions in parallel to the POP-1 pathway to specify endoderm (Maduro et al., 2005b). Depletion of *pop-1* in the *skn-1(zu67)* mutant background enhanced the *skn-1(zu67)* gutless phenotype from 64% to almost 100%. *sys-1(RNAi)* also enhanced the *skn-1(zu67)* gutless phenotype to 100% (n=68), consistent with SYS-1 functioning in the same pathway as POP-1 in endoderm specification.

Elevated POP-1 or reduced SYS-1 levels enhance the Mom phenotype, whereas elevated SYS-1 levels suppress it

sys-1(RNAi) produced a strong enhancement of the gutless phenotype in all *mom* mutants examined (Table 1). A striking example is the enhancement of *lit-1(t1534)* from 0% (n=116) to 100% (n=126) gutless. Conversely, we observed a strong suppression of the gutless phenotype in most *mom* mutants or RNAi embryos carrying a transgene expressing GFP::SYS-1 in either all [*teIs98(P$_{pie-1}$gfp::sys-1)*] or the EMS [*teEx321(P$_{med-1}$gfp::sys-1)*] lineages. For example, the penetrance of the Mom phenotype in *apr-1(RNAi)* and *mom-4(ne19)* embryos dropped from 29% (n=70) and 40% (n=65) to 0% (n=20) and 1% (n=67), respectively, in the *teEx321* background. Both these SYS-1 reduction-of-function and overexpression results suggest that the level of SYS-1 is important for endoderm specification.

An increase in the level of POP-1 also affects the penetrance of the gutless phenotype in *mom* mutants. Worms carrying extra copies of *pop-1* transgenes [*teIs3(P$_{med-1}$gfp::pop-1)*] expressing GFP::POP-1 in the EMS lineage display normal POP-1 nuclear asymmetry and no developmental defect (Lo et al., 2004). We observed a strong enhancement of the Mom phenotype with *teIs3* (Table 1), which increased the percentage of gutless embryos from 29% (n=70) and 43% (n=65) to 71% (n=62) and 75% (n=56), respectively, for *apr-*

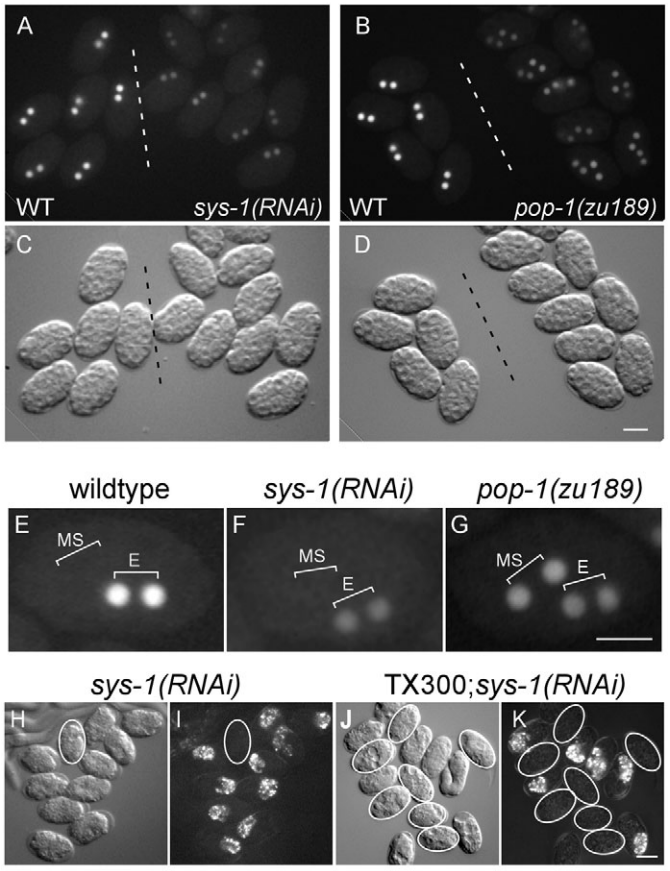

Fig. 1. SYS-1 is required for the activation of Wnt target genes in E and gut formation. (**A-D**) Micrographs of *C. elegans* embryos carrying the *Psdz-23::gfp::H2B* transgene, in wild-type, *sys-1(RNAi)* or *pop-1(zu189)* backgrounds. Embryos are shown at the two MS, two E stage, as DIC (C,D) and corresponding nuclear GFP::H2B fluorescence (A,B) images. Wild-type (left of the dashed line) and RNAi/mutant embryos (right of the dashed line) were imaged together. Note reduced GFP fluorescence in *sys-1(RNAi)* and *pop-1(zu189)* embryos as compared with wild-type embryos. Four GFP-positive cells were observed in *pop-1(zu189)* embryos owing to derepression in the MS lineage. (**E-G**) Representative wild-type, *sys-1(RNAi)* and *pop-1(zu189)* embryos from A-D showing reporter GFP expression. (**H-K**) Terminally differentiated *sys-1(RNAi)* (H,I) or *tels3($P_{med\text{-}1}$gfp::pop-1); sys-1(RNAi)* (J,K) embryos shown under DIC (H,J) or birefringence optics revealing intestinal-specific gut granules (white speckles in I,K). Embryos lacking gut granules are outlined in white. Scale bars: 20 μm.

1(RNAi) and *mom-4(ne19)*. This effect is similar to that observed for depletion of *sys-1* and opposite to that observed following an increase in SYS-1 levels. These results demonstrate that both POP-1 and SYS-1 levels are important for endoderm specification. A high level of SYS-1 promotes, whereas a low level of SYS-1 or a high level of POP-1 antagonizes, the endoderm fate.

teIs98($P_{pie\text{-}1}$gfp::sys-1) suppressed the gutless phenotype in *skn-1(RNAi)* embryos (Table 1), suggesting that the effect upon the gutless phenotype reflects an altered POP-1 activity and not an altered SKN-1-dependent pathway. The penetrance of the gutless phenotype dropped from 76% (n=163) in *skn-1(RNAi)* embryos to 16% (n=215) following *skn-1(RNAi)* in *teIs98*. This SKN-1-independent suppression was also observed in *mom-2(or42)* and *mom-5(or57)* mutant backgrounds (Table 1). Because expression of GFP::SYS-1 in *teEx321($P_{med\text{-}1}$gfp::sys-1)* depends on SKN-1

Table 1. Penetrance of gutless phenotype in various mutants with altered SYS-1 or POP-1 levels

	Reported	This study
skn-1(zu67)	67*	63 (46)†
sys-1 (RNAi)		4 (429)
skn-1(zu67); sys-1 (RNAi)		100 (68)
skn-1(RNAi)(inj)‡		74 (46)
skn-1(RNAi)		72 (163)
skn-1(RNAi)(inj); mom-2 (or42)	100§	100 (71)
skn-1(RNAi)(inj); mom-4 (ne19)		100 (79)
skn-1(RNAi); mom-5(or57)		96 (179)
teEx321($P_{med\text{-}1}$gfp::sys-1)¶		0 (134)
*tels3($P_{med\text{-}1}$gfp::pop-1)***		0 (150)
*tels98($P_{pie\text{-}1}$gfp::sys-1)***		0 (392)
skn-1(RNAi); teIs98		16 (215)
mom-1(or10)	85§	83 (55)
mom-1(or10); sys-1(RNAi)		93 (41)
mom-1(or10); tels3		93 (41)
mom-2(or42)	73§	72 (105)
mom-2(RNAi)	14‡‡	28 (49)
mom-2(or42); sys-1(RNAi)		100 (229)
mom-2(or42); teEx321		10 (39)
mom-2(RNAi)††; tels3		60 (67)
mom-2(or42); teIs98		28 (145)
mom-2(or42); teIs98; skn-1(RNAi)		94 (467)
mom-3(or78)	65§	70 (60)
mom-3(or78); sys-1(RNAi)		81 (80)
mom-3(or78); teEx321		13 (15)
mom-3(or78); tels3		84 (50)
mom-4(ne19)	43‡‡	40 (65)
mom-4(ne19); sys-1(RNAi)		100 (246)
mom-4(ne19); teEx321		1 (67)
mom-4(ne19); tels3		75 (56)
mom-5(or57)	5§	14 (113)
mom-5(or57); sys-1(RNAi)		60 (134)
mom-5(or57); teEx321		0 (62)
mom-5(or57); tels3		65 (93)
mom-5(or57); teIs98		4 (131)
mom-5(or57); teIs98; skn-1(RNAi)		52 (188)
apr-1(RNAi)	26‡‡	29 (70)
apr-1(RNAi); teEx321		0 (20)
apr-1(RNAi); tels3		71 (62)
lit-1(t1534)	0§§	0 (116)
lit-1(t1534); sys-1(RNAi)		100 (126)
lit-1(t1534); tels3		94 (56)
lit-1(1512)	100§§	99 (224)
lit-1(t1512); teEx321		65 (31)
wrm-1(RNAi)	100‡‡	100 (122)
wrm-1(RNAi); sys-1(RNAi)		100 (87)
wrm-1(RNAi); teEx321		100 (143)
wrm-1(RNAi); tels3		100 (170)
med-1/2(RNAi)¶¶	7-52	16 (61)
med-1/2(RNAi); mom-2(or42)		85 (66)
med-1/2(RNAi); mom-4(ne19)		46 (57)
med-1/2(RNAi); mom-2(or42); teEx321		23 (31)
med-1/2(RNAi); mom-4(ne19); teEx321		19 (27)

*(Bowerman et al., 1992).
†Numbers indicate percentage gutless. Numbers in parentheses indicate total number of embryos scored.
‡All *skn-1(RNAi)* was performed by feeding, except those indicated as injection *(inj)*.
§(Thorpe et al., 1997).
¶*teEx321* was crossed into adult mutant hermaphrodites and GFP-positive embryos were scored.
**Balanced *mom* mutant strains carrying *tels3 and teIs98* were generated. Embryos were collected from mutant hermaphrodites and scored for gut formation.
††*tels3* is on V, the same linkage group as *mom-2*, therefore *mom-2(RNAi)* was performed.
‡‡(Rocheleau et al., 1997).
§§(Kaletta et al., 1997).
¶¶7% gutless (Goszczynski et al., 2005). 52% gutless (Maduro et al., 2001). 6 mg/ml double-stranded *med-1/2* RNA was injected and embryos laid 24 hours post-injection were assayed for gut formation.

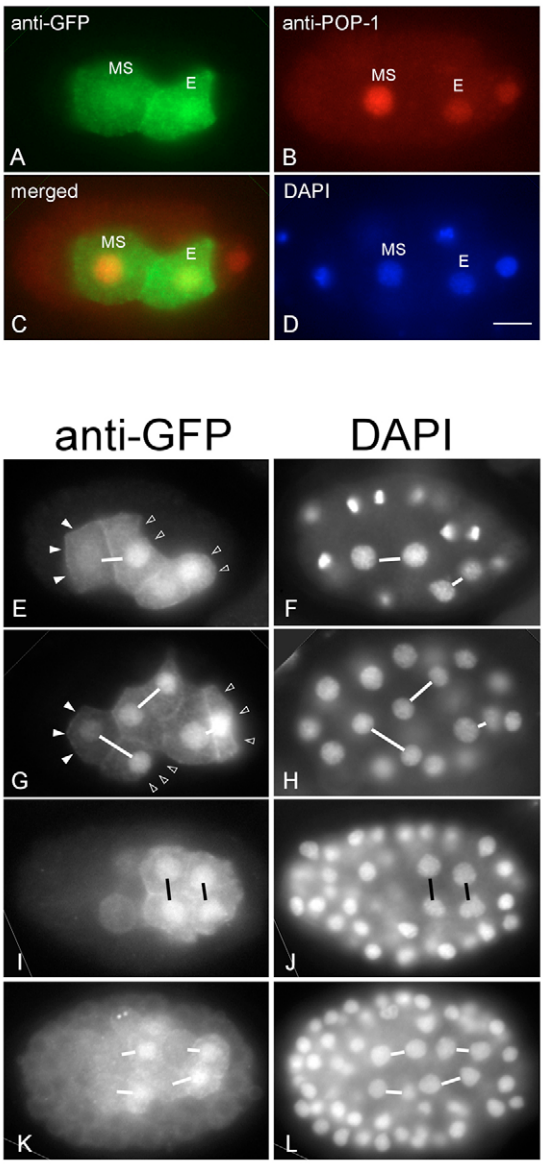

Fig. 2. Reciprocal nuclear asymmetry of GFP::SYS-1 and POP-1 between A-P sisters. Immunofluorescence micrographs of *teEx321($P_{med\text{-}1}$gfp::sys-1) C. elegans* embryos. (**A-D**) Embryos at 1MS/1E stage stained with (A) anti-GFP antibody, (B) anti-POP-1 mABRL2 and (D) DAPI to visualize nuclei. (C) Merged image. (**E-L**) Anti-GFP (left) and corresponding DAPI staining (right) at 2E stage (E-H), 4E stage (I,J) and 8E stage (K,L) of embryogenesis. White lines connect nuclei of sister cells born from A-P divisions; black lines connect nuclei born from left-right divisions. The cortical GFP signal often appeared asymmetric, being observed at the anterior cortex of anterior cells (white arrowheads) but not at the posterior cortex of posterior sisters (open arrowheads). Scale bar: 10 μm.

activity, we inactivated the SKN-1 pathway by RNAi of *med-1* and *med-2*, genes encoding transcription factors downstream of *skn-1*, as it has been shown that depletion of both *med-1* and *med-2* by RNAi results in gutless embryos (Maduro et al., 2001). We performed *med-1/2(RNAi)* in *mom-2(or42)*, *mom-4(ne19)*, *mom-2(or42); teEx321* and *mom-4(ne19); teEx321* embryos. In every case we examined, *teEx321* suppressed the gutless phenotype when *med-1* and *med-2* were depleted by RNAi (Table 1).

Genetic interaction between *pop-1* and *sys-1*

The low penetrance gutless phenotype observed following *sys-1(RNAi)* was enhanced by over 10-fold (59%, *n*=205) in the *teIs3($P_{med\text{-}1}$gfp::pop-1)* background (Fig. 1J,K). In addition, whereas *sys-1(q544)/+* animals produced no dead embryos, *sys-1(q544)/+; teIs3* produced 42% dead embryos and larvae (*n*=105), with 4% of these embryos being gutless. The increased severity of *sys-1* depletion in a genetic background in which the POP-1 level is elevated demonstrates that, although both POP-1 and SYS-1 absolute levels are important, their abundance relative to each other is more important for the specification of endoderm. A high SYS-1-to-POP-1 ratio promotes the endoderm fate.

Nuclear SYS-1 levels are higher in E than MS, reciprocal to nuclear POP-1

Localization of GFP::SYS-1 in the MS and E blastomeres and their descendants in *teEx321($P_{med\text{-}1}$gfp::sys-1)* embryos was determined by immunofluorescence using an anti-GFP antibody. We observed a dynamic subcellular localization of GFP::SYS-1 throughout the cell cycle (see Fig. S1 in the supplementary material), including centrosomal accumulation at metaphase. During interphase, we observed a higher overall level of nuclear and cytoplasmic GFP in E versus MS. It has also recently been reported that VENUS-tagged full-length SYS-1 associates with centrosomes and is at a higher level in E than in MS (Phillips et al., 2007). The GFP::SYS-1 asymmetry is reciprocal to POP-1 nuclear asymmetry (Lin et al., 1995) (Fig. 2A-D).

Similar to POP-1 asymmetry, the reciprocal GFP::SYS-1 asymmetry was also found to be reiterated in subsequent A-P divisions in the EMS lineage (Fig. 2E-L). MS and its descendents divide along the A-P axis five times during embryogenesis. By following the first three rounds of A-P divisions in the MS lineage in fixed embryos, we observed a higher level of cytoplasmic and nuclear GFP in all posterior cells compared with their anterior sisters (Fig. 2E-H; data not shown). E divides A-P then left-right, after which the four E descendents undergo several more rounds of A-P divisions to generate the entire intestine. We observed asymmetric GFP::SYS-1 in all A-P divisions of the E lineage (Fig. 2E-H,K-L). GFP::SYS-1 levels were observed to be equal only in the two pairs of sisters derived from the left-right divisions of Ea and Ep (Fig. 2I,J).

AB, the anterior blastomere of a 2-cell embryo, first undergoes a dorsal-ventral then a left-right division, before dividing anterior-posteriorly five times. In early *teIs98($P_{pie\text{-}1}$gfp::sys-1)* embryos, in which GFP::SYS-1 is expressed in all lineages, we observed GFP::SYS-1 asymmetry in all AB descendants that derived from A-P divisions that we could identify, including those generating 8, 16 and 32 AB cells (referred to as AB8, AB16 and AB32 cells). This reiterated reciprocal asymmetry of nuclear POP-1 and GFP::SYS-1 levels suggests that SYS-1 functions as a coactivator for POP-1 in the posterior cell following multiple A-P divisions in multiple lineages.

Differential regulation of SYS-1 and POP-1 A-P asymmetry by the Wnt and MAPK pathways

We depleted a component in the Wnt or MAPK pathways via genetic mutation or RNAi and assayed the effect in the EMS lineage. We scored the MSa/MSp and Ea/Ep pairs of sisters because stronger GFP::SYS-1 staining permitted easier scoring (Fig. 2E,F; Fig. 3Ba-c). GFP::SYS-1 asymmetry between MSa/MSp and Ea/Ep pairs of sisters was abolished or defective in most *mom-2(or42)*, *mom-5(RNAi)*, *mom-5(or57)* or *apr-1(RNAi)* embryos (Fig. 3Aa-d; 3Bd-

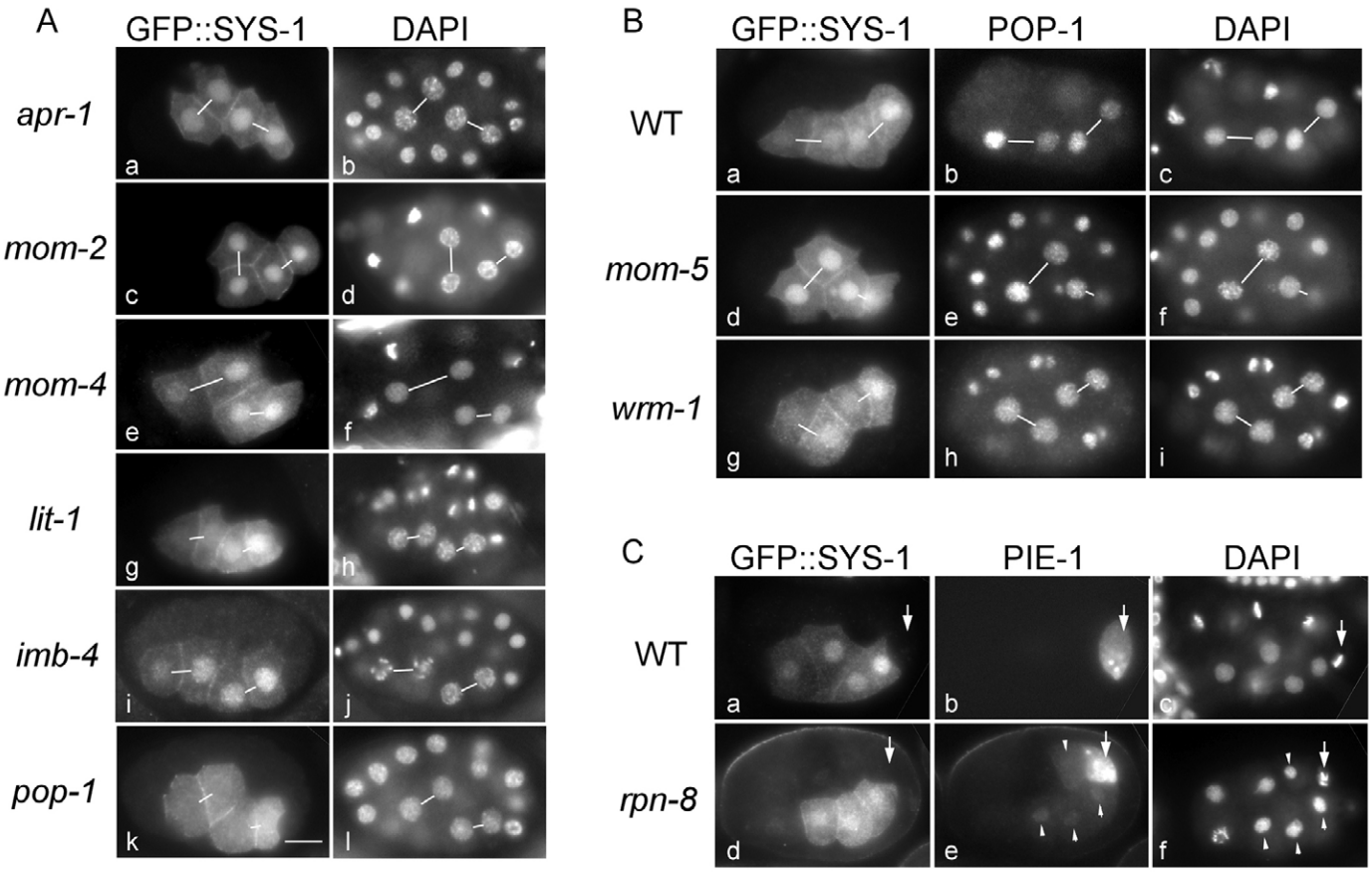

Fig. 3. GFP::SYS-1 nuclear asymmetry between A-P sisters is Wnt signal- and proteasome-dependent. Embryos are shown at the 2MS/2E stage, with lines connecting the MSa/MSp and Ea/Ep sisters. (**A**) Immunofluorescence micrographs of GFP::SYS-1 in various mutant backgrounds (as indicated to the left). Left column, anti-GFP; right column, DAPI. (**B**) Independent regulation of GFP::SYS-1 (a,d,g) and POP-1 (b,e,h) asymmetry. (a-c) Wild type; (d-f) *mom-5(or57)* showing symmetric GFP::SYS-1 and asymmetric POP-1; (g-i) *wrm-1(RNAi)* showing asymmetric GFP::SYS-1 and symmetric POP-1. (**C**) Wild-type (a-c) and *rpn-8(RNAi)* (d-f) embryos double stained with antibodies to GFP and PIE-1. Arrow, germline precursor; arrowheads, somatic nuclei that stain weakly with the PIE-1 antibody. Scale bar: 10 μm.

f; Table 2). Double staining with anti-POP-1 antibody also showed subtle defects in nuclear POP-1 asymmetry, although the POP-1 asymmetry defect tended to be less penetrant, with some asymmetry often still observed between sister blastomeres (Table 2). Both GFP::SYS-1 and nuclear POP-1 asymmetries were restored in these mutants following the 2E/4MS stage. Conversely, we observed no or very little defect in GFP::SYS-1 asymmetry in *mom-4(ne19)*, *lit-1(RNAi)*, *lit-1(t1512)* or *wrm-1(RNAi)* embryos, despite a complete abolishment of POP-1 asymmetry (Fig. 3Ae-h; 3Bg-i; Table 2).

We also scored the effect of *wrm-1*, *mom-2* and *mom-5* depletion on GFP::SYS-1 in AB8 and AB16 cells (Table 2). In both *mom-2(or42)* and *mom-5(or57)* mutants (n=5 and 6, respectively), we

Table 2. Defects in POP-1 and GFP::SYS-1 asymmetry in various genetic backgrounds

	MSa/MSp		Ea/Ep		AB8		AB16		AB32	
	SYS-1*	POP-1	SYS-1	POP-1	SYS-1	POP-1	SYS-1	POP-1	SYS-1	POP-1
Wild-type N2	1 (132)†	5 (131)	1 (79)	9 (75)	0 (7)	0 (7)	0 (18)	0 (18)	0 (6)	0 (6)
mom-2(or42)	100 (26)	100‡ (26)	79 (33)	76 (33)	100 (5)	40 (5)	17 (12)	0 (12)	0 (2)	0 (2)
mom-5(or57)	100 (6)	86 (7)	100 (8)	87 (8)	100 (6)	88 (6)	65 (17)	59 (17)	11 (9)	11 (9)
apr-1(RNAi)	100 (15)	100 (14)	93 (14)	87 (15)						
lit-1(t1512)	0 (19)	100 (19)	22 (9)	100 (9)						
mom-4(ne19)	0 (16)	100 (16)	0 (19)	100 (19)						
wrm-1(RNAi)	0 (37)	100 (37)	0 (20)	100 (20)	0 (6)	100 (6)	0 (10)	100 (10)	0 (3)	100 (3)
wrm-1(ne1982)	11 (19)§	53 (19)	0 (22)	32 (22)						

*SYS-1 was scored by immunofluorescence using the anti-GFP antibody in *teEx321* and *teIs98* embryos.
†Numbers indicate percentage of sister pairs scored with abnormal asymmetry. Numbers in parenthesis are total number of pairs scored. Abnormal asymmetry is defined as a pattern different from wild type. Sister pairs with only subtle differences were scored as abnormal. For AB8, AB16 and AB32, abnormality was scored if some or all pairs of AB cells at that particular stage were scored as abnormal.
‡Most pairs of sister cells scored as having abnormal POP-1 asymmetry in *mom-2*, *mom-5* and *apr-1* embryos, still had subtle POP-1 asymmetry.
§We observed abnormal SYS-1 asymmetry between the MSa/MSp pair in two *ne1982* embryos. One embryo had only a subtle difference between MSa and MSp, whereas the other had a reversed asymmetry.

observed a 100% loss of GFP::SYS-1 asymmetry in AB8 cells. This asymmetry defect decreased by the AB16 and AB32 stages to 17% and 0% (n=12) for *mom-2(or42)*, and 65% and 11% (n=17) for *mom-5(or57)* embryos, respectively. The defect for nuclear POP-1 asymmetry was less penetrant at the same stages (Table 2). In *wrm-1(RNAi)* embryos, despite a fully penetrant defect for nuclear POP-1 asymmetry, we detected no loss of GFP::SYS-1 asymmetry in AB8, AB16 or AB32 cells (n=6, 10 and 3, respectively). Taken together, our results demonstrate that genes regulating endoderm specification contribute differentially to SYS-1 and POP-1 asymmetry. GFP::SYS-1 asymmetry is regulated by *mom-2*, *mom-5* and *apr-1*, but not by *mom-4*, *lit-1* or *wrm-1*. On the contrary, *mom-4*, *lit-1* and *wrm-1* influence nuclear POP-1 asymmetry much more than do *mom-2*, *mom-5* and *apr-1*.

Depletion of *pop-1* (*zu189* or *RNAi)* resulted in a decrease in GFP::SYS-1 nuclear staining and a concomitant increase in cytoplasmic signal in all expressing cells, without abolishing the differential GFP levels between A-P sisters (Fig. 3Ak,l; data not shown), suggesting that POP-1 regulates nuclear localization or nuclear retention of SYS-1.

SYS-1 asymmetry is dependent on the proteasome but not nuclear export

Is GFP::SYS-1 asymmetry regulated, as it is for POP-1, via nuclear export? Three genes, *imb-4*, *ran-3* and *ran-4*, which have been shown to function in nuclear export, were individually depleted by RNAi in *teEx321($P_{med\text{-}1}$gfp::sys-1)*. All (n=18) *imb-4(RNAi)* and ~50% of *ran-3(RNAi)* and *ran-4(RNAi)* embryos (n=15 and 11, respectively) exhibited exclusively nuclear GFP::SYS-1, consistent with these three genes functioning in GFP::SYS-1 nuclear export. However, GFP::SYS-1 levels were still observed to be different between A-P sisters in all embryos depleted of any of these three genes (Fig. 3Ai,j; data not shown). This result, and the cytoplasmic GFP::SYS-1 observed in *pop-1* mutant embryos, suggest that neither nuclear export nor differential subcellular distribution accounts for the GFP::SYS-1 asymmetry between A-P sisters.

GFP::SYS-1 asymmetry is lost, however, by depletion of components of the proteasome. When three components of the proteasome, *rpn-8*, *pas-4*, *pbs-2* were individually depleted, we observed in each case a similar level of GFP::SYS-1 in almost all GFP-expressing blastomeres (Fig. 3Cd; data not shown). This loss of GFP::SYS-1 asymmetry is not due to a loss of embryonic polarity in RNAi embryos per se. PIE-1 in wild-type embryos is localized to germ cell precursors (Fig. 3Ca-c) (Mello et al., 1996), which requires proper establishment of embryonic polarity and proteasome-mediated degradation of PIE-1 segregated to somatic cells (DeRenzo et al., 2003). Under our RNAi conditions, we detected in all cases (n=6) GFP::SYS-1 equally distributed between A-P sister blastomeres, and PIE-1 primarily in the germline precursor (Fig. 3Cd-f). We also detected a small amount of PIE-1 in somatic cells, consistent with a defect in proteasome-mediated degradation in these RNAi embryos. These results argue that GFP::SYS-1 asymmetry is regulated via proteasomal degradation.

Elevated SYS-1 expression results in an MS-to-E fate transformation

Approximately 50% (n=71) of GFP-positive *teEx321($P_{med\text{-}1}$gfp::sys-1)* embryos either failed to hatch or died as L1 larvae. Immunofluorescence analyses detected no embryos lacking gut (n>1000). Instead, we observed a small number of embryos (3%, n>500) with approximately twice the number of intestinal cells and missing the posterior pharynx (Fig. 4). This phenocopies *pop-1(zu189)* mutant embryos (Lin et al., 1995), consistent with an MS-to-E fate transformation.

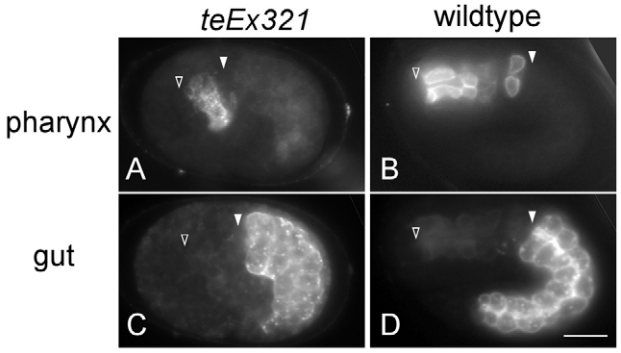

Fig. 4. Increased level of SYS-1 causes extra gut at the expense of pharynx. Immunofluorescence of *teEx321($P_{med\text{-}1}$gfp::sys-1)* (**A**,**C**) and wild-type (**B**,**D**) *C. elegans* embryos stained with 3NB12 for pharynx (A,B) or ICB4 for gut (C,D). The anterior and posterior tips of the pharynx are indicated by open and closed arrowheads, respectively. Scale bar: 10 μm.

This *pop-1* phenocopy was greatly enhanced following mild reduction of *pop-1* by RNAi. Under *pop-1* RNAi conditions in which two control strains, N2 and *teIs18($P_{sdz\text{-}23}$gfp::H2B)* (Shetty et al., 2005), produced only 13% (n=82) and 29% (n=104) *pop-1*-like embryos, respectively, *teEx321($P_{med\text{-}1}$gfp::sys-1)* GFP-positive embryos produced 75% (n=49) *pop-1*-like embryos. As elevated SYS-1 levels result in an MS-to-E fate transformation, this result strongly suggests that the SYS-1 level is limiting with respect to POP-1 in MS, precluding MS from making endoderm.

The SYS-1-to-POP-1 ratio is also critical for other A-P divisions

The SYS-1-to-POP-1 ratio regulates reiterating, asymmetric cell fate changes at other A-P divisions within the MS and E lineages.

The MS lineage

The *C. elegans* pharynx consists of eight muscle types (pm1 through pm8) arranged as eight consecutive rings with three cells in each ring (Fig. 5A) (Albertson and Thomson, 1976). An antibody, 3NB12, recognizing pm3, pm4, pm5 and pm7 cells, generates a characteristic staining gap in wild-type pharynx between pm5 and pm7, owing to the inability of this antibody to stain pm6 cells (Fig. 5B) (Priess and Thomson, 1987).

The three pm6 and three pm7 cells are all derived from the MS lineage. One pm6 and two pm7 cells are derived from MSa, whereas two pm6 and a single pm7 cell are derived from MSp (Sulston et al., 1983). Based upon the known lineage, an MSa-to-MSp fate change would be predicted to result in the MSa-derived pm6 cell (**MSa**apappa) and the MSa-derived pm7 cells (**MSa**aaappp and **MSa**apaapp) adopting the fate of **MSp**apappa, **MSp**aaappp and **MSp**apaapp, respectively (see Table S1 in the supplementary material). The net result would be the absence of one 3NB12-positive pm7 cell and the presence of one additional 3NB12-negative pm6 cell at the terminal bulb. The same lineage calculations for an MSp-to-MSa fate change predict one additional 3NB12-positive pm7 muscle cell and the absence of one 3NB12-negative pm6 muscle cell (Fig. 5B and see Table S1 in the supplementary material).

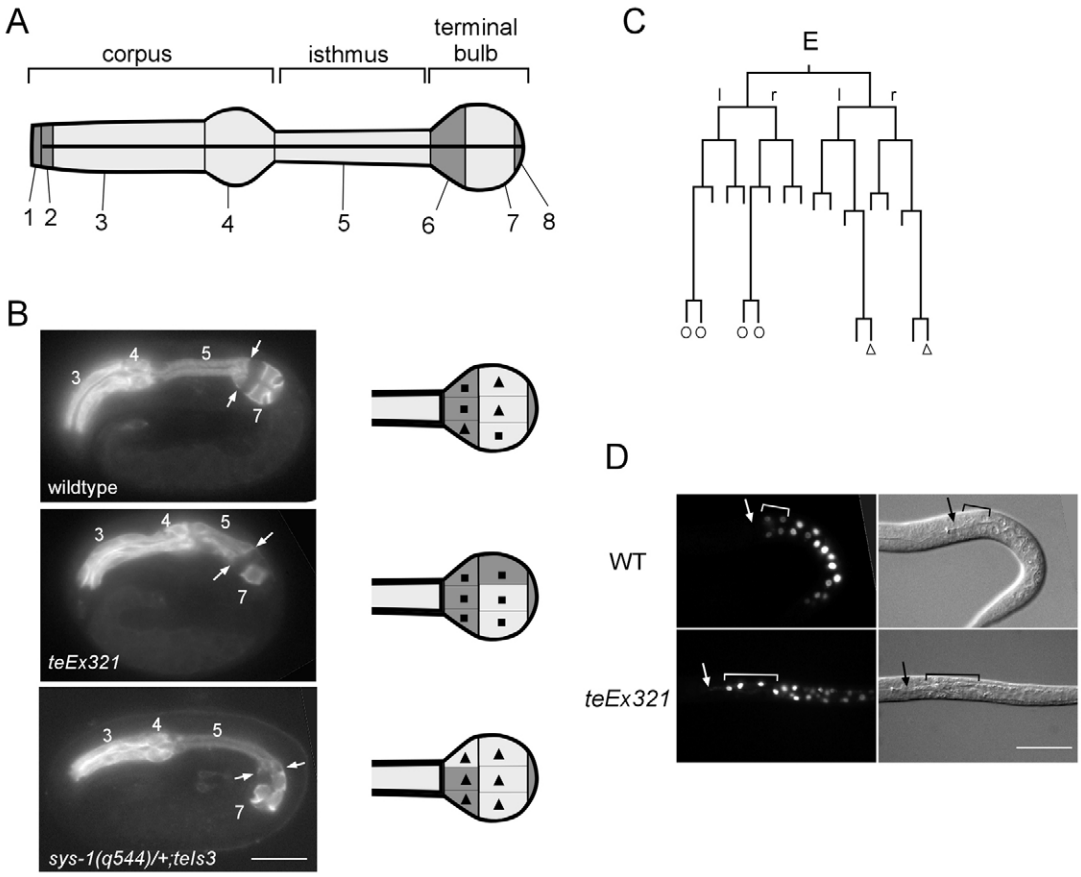

Fig. 5. Altering the SYS-1-to-POP-1 ratio also affects cell fate decisions at other A-P divisions. (**A**) Schematic of the *C. elegans* pharynx, including the location of the eight pharyngeal muscle types (labeled 1 through 8), with 3NB12 staining indicated (dark gray, no staining). (**B**) Embryos derived from wild type, *teEx321*($P_{med\text{-}1}$*gfp::sys-1)* and *sys-1(q544/+); teIs3*($P_{med\text{-}1}$*gfp::pop-1)* stained with 3NB12. Schematics to the right indicate the three pm6 and three pm7 muscle cells in the wild type and predicted cell fate changes following an anterior-to-posterior (middle) or a posterior-to-anterior (bottom) fate transformation at the division giving rise to MSa and MSp. Triangles and squares denote cells derived from the MSa and MSp lineages, respectively. (**C**) The E lineage. Horizontal lines indicate divisions, whereas vertical lines indicate developmental time. All divisions are anterior (left) to posterior (right), except those labeled l/r, which indicate left/right divisions. Circles, the four cells that comprise intestinal ring 1; triangles, the two cells comprising ring 9. (**D**) PHO-1::GFP expression in wild-type and *teEx321* larvae. Arrow, posterior end of the pharynx; brackets, cells in the first two intestinal rings in wild type and the corresponding region in *teEx321*. Scale bar: 10 μm in B; 30 μm in D.

Approximately 10% (*n*=1000) of the *teEx321*($P_{med\text{-}1}$*gfp::sys-1)* embryos exhibited a decrease in the number of pm7 muscle cells upon 3NB12 staining (Fig. 5B). Instead of the three pm7 cells always observed in wild-type embryos, we often observed only two pm7 cells in *teEx321* embryos. On the contrary, ~10% of embryos and larvae derived from *sys-1(q544/+); teIs3*($P_{med\text{-}1}$*gfp::pop-1)* had four 3NB12-positive cells and a smaller area than in the wild type unstained by 3NB12 in the terminal bulb (Fig. 5B). We did not observe any *teEx321* embryos with extra pm7 muscle cells or progeny of *sys-1(q544/+); teIs3* with missing pm7 muscle cells (*n*>1000). Although we cannot be certain that an extra pm7 cell is generated at the expense of a pm6 cell, or that a missing pm7 cell has become a pm6 cell, the phenotype observed for *teEx321* is consistent with the lineage prediction for an MSa-to-MSp fate change. Likewise, the *sys-1(q544/+); teIs3* phenotype is consistent with the predicted MSp-to-MSa fate change.

The E lineage

The entire 20-cell intestine is clonally derived from the E blastomere and is arranged in nine sequential rings (Fig. 5C) (Sulston et al., 1983). The four cells that comprise ring 1 are two pairs of sisters (Ealaaa and Ealaap, Earaaa and Earaap), which derive from the most anterior lineage of Eal and Ear, respectively (Fig. 5C). These cells would be the most sensitive to any anterior-to-posterior fate transformation within the E lineage. All fate transformations within the E lineage should still give rise to intestinal cells. Fortunately, intestinal cells that derive from different branches of the E lineage exhibit different properties (Fukushige et al., 2005; Schroeder and McGhee, 1998). For example, the gut phosphoesterase PHO-1, which is expressed strongly in all other gut cells, is expressed weakly in the six cells that make up the first two intestinal rings (Fig. 5D) (Fukushige et al., 2005). We observed that 100% (*n*=22) of *teEx321*($P_{med\text{-}1}$*gfp::sys-1)* GFP-positive progeny exhibited bright PHO-1 reporter GFP fluorescence in at least some of the four anterior-most intestinal cells, compared with 0% (*n*=10) of wild-type embryos (Fig. 5D). The first gut ring is also responsible for attaching intestine anteriorly to the pharyngeal/intestinal valve cells. We observed ~13% (*n*=71) of *teEx321* GFP-positive progeny with intestine unattached to the pharynx (not shown). These results are consistent with lineage defects among the cells comprising ring 1. In addition, MSa also gives rise to the pm8 muscle cell, which attaches the pharynx to the pharyngeal/intestinal valve cells (Sulston

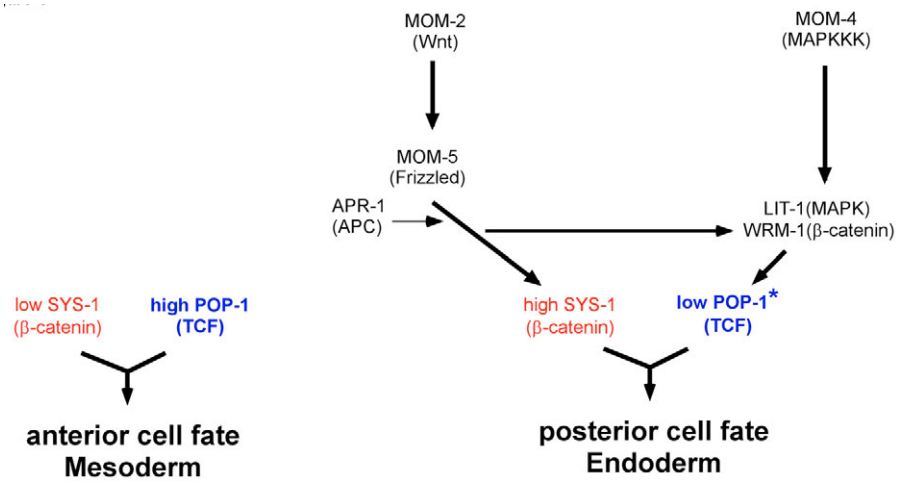

Fig. 6. Pathways regulating the reciprocal asymmetry of POP-1 and SYS-1 in *C. elegans*. Schematic of the two pathways regulating nuclear SYS-1 and POP-1 levels. SYS-1 levels are elevated by the MOM-2/MOM-5/APR-1 pathway, and nuclear POP-1 levels are decreased by the MOM-4/WRM-1/LIT-1 pathway with input from the MOM-2/MOM-5/APR-1 pathway. Each pathway contributes to an increase in the SYS-1-to-POP-1 ratio, which drives the posterior cell fate. The asterisk denotes that POP-1 activity could be regulated via post-translational modification.

et al., 1983). Therefore, pm8 lineage defects could also contribute to the unattached anterior intestine phenotype observed in *teEx321* progeny.

The most-posterior gut ring, composed of two cells (Eplppp and Eprppp), attaches intestine to the intestinal/rectal valve cells. These cells, born as the most posterior lineage of Epl and Epr, respectively (Fig. 5C) (Sulston et al., 1983), would be the most sensitive to any posterior-to-anterior fate transformation within the E lineage. In 23% (n=105) of larvae derived from *sys-1(q544/+); teIs3($P_{med\text{-}1}$gfp::pop-1)*, the posterior of the intestine was not attached to the rectum (not shown). No defect in intestinal attachment to pharynx was observed (n>1000). Similarly, no defect in intestinal attachment to rectum was observed in *teEx321($P_{med\text{-}1}$gfp::sys-1)* embryos (n>1000). Staining with antibody ICB4 (Kemphues et al., 1988) showed that, although the majority of embryos derived from *teEx321* and *sys-1(q544/+); teIs3* had a disorganized intestine, they had twenty, or close to twenty, intestinal cells (n=50).

Together, our results show that a high SYS-1-to-POP-1 ratio inhibits the anterior cell fate, whereas a low ratio inhibits the posterior fate in multiple A-P divisions during *C. elegans* embryogenesis.

DISCUSSION

We show in this study that the β-catenin SYS-1 functions as a limiting coactivator for the TCF protein POP-1 in activating Wnt/MAPK-responsive genes in the endoderm precursor. More importantly, we show that the SYS-1-to-POP-1 ratio appears critical for both the anterior and posterior cell fates in multiple asymmetric divisions regulated by Wnt/MAPK signaling: a high ratio drives the posterior cell fate, whereas a low ratio drives the anterior cell fate. In posterior cells, GFP::SYS-1 levels are elevated, whereas nuclear POP-1 levels are lowered. Our results demonstrate that the MOM-2/MOM-5/APR-1 and MOM-4/LIT-1/WRM-1 pathways, by virtue of their differential effects on SYS-1 and POP-1 nuclear levels, mutually reinforce an increase in the SYS-1-to-POP-1 ratio in posterior cells, thereby robustly promoting A-P cell fate asymmetries (Fig. 6). As *C. elegans* embryogenesis consists primarily of a series of binary cell fate specifications at A-P divisions, the reiteration of this mechanism may drive much of the invariant lineage.

SYS-1 functions as a limiting coactivator for POP-1 in the E blastomere

Nuclear POP-1 asymmetry has been observed in several asymmetric A-P sisters whose differential cell fates require MAPK and/or Wnt signaling (Herman, 2001; Lin et al., 1998; Lin et al., 1995; Siegfried et al., 2004). Signaling and POP-1 activation are required for the posterior cell fate and in all cases these cells have a lower level of nuclear POP-1 (Herman, 2001; Maduro et al., 2005b; Shetty et al., 2005; Siegfried and Kimble, 2002). The requirement for lowered levels of nuclear POP-1 in cells in which POP-1 functions as an activator suggested a model invoking a co-activator for POP-1, the amount of which is limiting with respect to POP-1 (Herman, 2001; Kidd et al., 2005; Shetty et al., 2005; Siegfried et al., 2004; Phillips et al., 2007). In cells with high nuclear POP-1 levels, only a small portion of POP-1 would be bound to the limiting co-activator, with the majority free to bind to co-repressor(s) resulting in transcriptional repression of target genes. In addition, POP-1 could be qualitatively different between asymmetric sisters, also promoting preferential interaction of POP-1 with co-activator in Wnt/MAPK-responsive cells.

We show here that the β-catenin SYS-1, like the TCF protein POP-1, is important for endoderm fate. Our data argue that the SYS-1-to-POP-1 ratio, more so than the absolute SYS-1 and POP-1 levels, is critical in E blastomere fate specification. A high SYS-1-to-POP-1 ratio promotes, whereas a low SYS-1-to-POP-1 ratio antagonizes, E fate. In the most convincing demonstration, simply increasing SYS-1 levels by introducing extra copies of *gfp::sys-1* was sufficient to transform MS blastomere fate to endoderm, or E fate. These results strongly support the model that SYS-1 levels are limiting with respect to POP-1 levels in the specification of endoderm fate.

Activation of Wnt target genes by coordinate regulation of β-catenin/SYS-1 and TCF/POP-1

A high SYS-1-to-POP-1 ratio can be achieved by decreasing the level of POP-1, increasing the level of SYS-1, or both. Our results demonstrate that GFP::SYS-1 and POP-1 levels are simultaneously regulated in opposite directions. Whereas the MOM-4/LIT-1/WRM-1 pathway plays the major role in lowering nuclear POP-1 levels, GFP::SYS-1 asymmetry is regulated primarily by the MOM-2/MOM-5/APR-1 pathway, with very little or no input from *wrm-1*, *lit-1* or *mom-4* (Fig. 6). These observations offer an explanation for the synergy observed by us and others between mutations in these two groups of genes: whereas *mom-2*, *mom-5* and *mom-4* mutations alone have an incompletely penetrant gutless phenotype, *mom-2; mom-4* and *mom-5; mom-4* embryos have a 100% gutless phenotype (Rocheleau et al., 1997; Rocheleau et al., 1999; Thorpe et al., 1997). Defects in altering the level of either SYS-1 or POP-1 alone would not result in as dramatic a change of the SYS-1-to-POP-1 ratio as

defects in altering both. Consistent with our results, Phillips et al. have recently shown that SYS-1 asymmetry in somatic gonad precursors is MOM-5-dependent, but LIT-1- and WRM-1-independent (Phillips et al., 2007). *lit-1* or *wrm-1* mutants, unlike *mom-4* mutants, produce 100% gutless embryos. It is possible that the LIT-1/WRM-1 kinase regulates POP-1 transcriptional activity, in addition to its role in regulating POP-1 nuclear levels. Supporting this possibility, phosphorylation of TCF proteins by nemo-like kinase (NLK) has been reported to inhibit the DNA-binding activity of TCFs (Ishitani et al., 2003) and to enhance transcription of Wnt targets (Thorpe and Moon, 2004). We propose that these two pathways specify endoderm fate by collaborating to very efficiently elevate the SYS-1-to-POP-1 ratio in the E blastomere. Furthermore, we propose that this redundancy helps to insulate a genetic system used in multiple A-P divisions during *C. elegans* embryogenesis from deleterious mutations, as well as ensuring that cell fate decisions are robust in a rapidly dividing embryo that nevertheless maintains an invariant lineage.

Studies in *Drosophila* also suggest that the β-catenin/TCF ratio can play an important role in Wnt signaling. *wingless* and *armadillo* (*arm*) mutant phenotypes can be partially suppressed by a reduction in *Drosophila* TCF (dTCF; also known as PAN – Flybase) activity, whereas the phenotype of a weak *wingless* allele is enhanced by overexpression of wild-type dTCF (Cavallo et al., 1998). It appears, therefore, that lower levels of dTCF, or higher levels of ARM, analogous to what we show here, contribute to Wnt signal strength. However, whereas regulation of β-catenin levels by Wnt is well documented in vertebrates and *Drosophila*, possible regulation of TCF levels by the MAPK pathway is less well documented. A recent report that NLK promotes TCF degradation by facilitating its interaction with an E3 ligase (Yamada et al., 2006), suggests that simultaneous regulation of β-catenin and TCF levels in opposite directions might not be unique to the *C. elegans* embryo.

The two β-catenins, WRM-1 and SYS-1

It has been suggested that the cellular functions carried out by a single β-catenin in vertebrates and flies are carried out by multiple β-catenins in worms (Korswagen et al., 2000). β-catenin has been shown to undergo importin-independent nuclear import, perhaps by directly binding to the nuclear pore complex through its armadillo repeats, which resemble the heat repeats of importin (Fagotto et al., 1998). β-catenin nuclear localization has been shown to then facilitate nuclear import of LEF1 and TCF4 by direct binding (Asally and Yoneda, 2005; Hsu et al., 2006). It is possible that WRM-1 is a specialized β-catenin that functions as a nuclear import receptor for LIT-1, or additional factors, in response to Wnt/MAPK signaling during *C. elegans* embryogenesis.

It is interesting that two β-catenins in *C. elegans*, SYS-1 and WRM-1, both function in endoderm precursor specification, exhibit an elevated level in the posterior cell of all A-P divisions, function in elevating the SYS-1-to-POP-1 ratio, have seemingly very different biological activities and are regulated through different mechanisms. Our current data are consistent with SYS-1 A-P asymmetry being regulated by differential degradation between sister cells. This resembles the downregulation of vertebrate β-catenins in the absence of Wnt signaling (Krieghoff et al., 2006), but is different from the situation for WRM-1, the asymmetric levels of which are dependent on IMB-4-mediated nuclear export (Nakamura et al., 2005). Recent work has shown that cortically localized WRM-1 represses its nuclear accumulation (Mizumoto and Sawa, 2007). It is interesting to note that GFP::SYS-1 also localized to centrosomes and differentially localized to cortex. However, the functional significance, if any, of centrosomal and cortical SYS-1 localization requires further investigation.

Pathways regulating endoderm

Analyses of the expression of the endoderm-specifying genes, *end-1* and *end-3*, demonstrated that both the SKN-1/MED-1 and the POP-1 (and now SYS-1) pathways contribute to the high level expression of these endoderm genes (Maduro et al., 2005b; Shetty et al., 2005). We propose that transcriptional activation of *end-1* and *end-3* by either the SKN-1/MED-1 or POP-1/SYS-1 pathway alone is sufficient to specify endoderm. In MS, where the SYS-1-to-POP-1 ratio is low, POP-1, in conjunction with co-repressor(s), overrides transcriptional activation by SKN-1/MED-1, resulting in no *end-1* or *end-3* expression and a lack of endoderm fate. In E, a high SYS-1-to-POP-1 ratio allows POP-1 to function as an activator, further elevating *end-1* and *end-3* transcription. Embryos with reduced expression of *end-1* and *end-3* as a result of *skn-1* depletion would be expected to be sensitive to alterations in the SYS-1-to-POP-1 ratio, consistent with the observed synergy between *skn-1* and *mom-2*, *mom-4* or *mom-5* mutations (Thorpe et al., 1997), and the suppression of *skn-1(zu67)* by *teIs98*($P_{pie\text{-}1}$*gfp::sys-1)* (this study).

SYS-1 and POP-1 function in MS

POP-1 is also required for MS fate specification. However, the role of POP-1 in MS specification is not simply repression of endoderm fate. In embryos in which the endoderm-specifying genes *end-1* and *end-3*, as well as *pop-1*, are deleted, the MS blastomere generates neither pharynx nor intestine (Maduro et al., 2005a; Zhu et al., 1997). This indicates that POP-1 plays an important and direct role in specifying MS fate, independent of its function in endoderm gene repression. We reported previously that in a large percentage of embryos with artificially elevated nuclear POP-1 levels in E, E also generates neither pharynx nor intestine (Lo et al., 2004). Therefore, a high level of nuclear POP-1 in E, although sufficient to repress endoderm, is not always sufficient to promote mesoderm. A low level (but not complete absence) of SYS-1 and a high level of nuclear POP-1 would appear to be important for the activation of genes specifying the MS blastomere. Other factors in addition to SYS-1 might also act with POP-1 to specify MS fate. A candidate for such a factor is the T-box protein, TBX-35, which has recently been shown to regulate MS-derived cell fates (Broitman-Maduro et al., 2006). Future studies will elaborate the roles of POP-1, SYS-1, TBX-35 and other factors in MS fate specification.

SYS-1 and POP-1 function in reiterated A-P cell fate decisions

We show that in multiple A-P divisions, a low SYS-1-to-POP-1 ratio promotes the anterior cell fate, whereas a high SYS-1-to-POP-1 ratio promotes the posterior fate. This suggests that the SYS-1-to-POP-1 ratio might have a broad role in controlling stepwise A-P binary decisions throughout *C. elegans* embryogenesis. However, we did not observe the collapse of the affected lineage to either the anterior-most or posterior-most cell fate by overexpressing or removing SYS-1 or POP-1. We anticipated that all transgenic strains isolated expressing altered levels of SYS-1 and/or POP-1 were likely to have a non-fully penetrant defect in all divisions in which these proteins might function. Full collapse of affected lineages would be expected to be 100% lethal and therefore not able to be isolated as a strain. In addition, for transgenes utilizing the *med-1* promoter to drive expression in the E and MS lineages, transcription only occurs early in the lineage (Maduro et al., 2001; Robertson et al., 2004).

Therefore, there is expected to be a progressive decrease in GFP::SYS-1 levels and a less severely altered SYS-1-to-POP-1 ratio as the embryo develops. It is also possible that the SYS-1-to-POP-1 ratio might regulate only a subset of cell divisions, despite exhibiting asymmetric levels in all A-P divisions.

Although asymmetric SYS-1 and nuclear POP-1 levels in AB8 cells are dependent on Wnt/MOM-2, some of these AB cells do not contact P2 or its descendants, which are the only cells that have been shown to be Wnt signaling cells at this stage. It has recently been proposed that Wnt signaling from P2 and its descendants can influence the polarity of blastomeres that they do not directly contact, because Wnt signaling can be passed on from cell to cell (Bischoff and Schnabel, 2006). However, the question remains: what initiates and regulates the asymmetry for both POP-1 and SYS-1 after the AB8 stage, as both occur in *mom-2* mutant embryos. Future studies involving blastomere isolation and reassociation will be required to address this question.

We thank members of the Lin laboratory for their useful comments, Jim McGhee, Jie Yan, Judith Kimble and Julie Ahringer for reagents, Judith Kimble and Jeff Hardin for sharing unpublished results, and Bruce Bowerman and Tim Schedl for useful discussions. This work was supported by the NIH, American Cancer Society and the American Heart Association (to R.L.).

Supplementary material

Supplementary material for this article is available at http://dev.biologists.org/cgi/content/full/134/14/2685/DC1

References

Albertson, D. G. and Thomson, J. N. (1976). The pharynx of Caenorhabditis elegans. *Philos. Trans. R. Soc. Lond. B Biol. Sci.* **275**, 299-325.

Asally, M. and Yoneda, Y. (2005). Beta-catenin can act as a nuclear import receptor for its partner transcription factor, lymphocyte enhancer factor-1 (lef-1). *Exp. Cell Res.* **308**, 357-363.

Bischoff, M. and Schnabel, R. (2006). A posterior center establishes and maintains polarity of the Caenorhabditis elegans embryo by a Wnt-dependent relay mechanism. *PLoS Biol.* **4**, 2262-2273.

Bowerman, B., Eaton, B. A. and Priess, J. R. (1992). skn-1, a maternally expressed gene required to specify the fate of ventral blastomeres in the early C. elegans embryo. *Cell* **68**, 1061-1075.

Broitman-Maduro, G., Lin, K. T.-H., Hung, W. W. K. and Maduro, M. F. (2006). Specification of the C. elegans MS blastomere by the T-box factor TBX-35. *Development* **133**, 3097-3106.

Calvo, D., Victor, M., Gay, F., Sui, G., Luke, M. P., Dufourcq, P., Wen, G., Maduro, M., Rothman, J. and Shi, Y. (2001). A POP-1 repressor complex restricts inappropriate cell type-specific gene transcription during Caenorhabditis elegans embryogenesis. *EMBO J.* **20**, 7197-7208.

Cavallo, R. A., Cox, R. T., Moline, M. M., Roose, J., Polevoy, G. A., Clevers, H., Peifer, M. and Bejsovec, A. (1998). Drosophila Tcf and Groucho interact to repress Wingless signalling activity. *Nature* **395**, 604-608.

Costa, M., Raich, W., Agbunag, C., Leung, B., Hardin, J. and Priess, J. R. (1998). A putative catenin-cadherin system mediates morphogenesis of the Caenorhabditis elegans embryo. *J. Cell Biol.* **141**, 297-308.

DeRenzo, C., Reese, K. J. and Seydoux, G. (2003). Exclusion of germ plasm proteins from somatic lineages by cullin-dependent degradation. *Nature* **424**, 685-689.

Eisenmann, D. M., Maloof, J. N., Simske, J. S., Kenyon, C. and Kim, S. K. (1998). The beta-catenin homolog BAR-1 and LET-60 Ras coordinately regulate the Hox gene lin-39 during Caenorhabditis elegans vulval development. *Development* **125**, 3667-3680.

Fagotto, F., Gluck, U. and Gumbiner, B. M. (1998). Nuclear localization signal-independent and importin/karyopherin-independent nuclear import of beta-catenin. *Curr. Biol.* **8**, 181-190.

Fukushige, T., Goszczynski, B., Yan, J. and McGhee, J. D. (2005). Transcriptional control and patterning of the pho-1 gene, an essential acid phosphatase expressed in the C. elegans intestine. *Dev. Biol.* **279**, 446-461.

Goldstein, B. (1992). Induction of gut in Caenorhabditis elegans embryos. *Nature* **357**, 255-257.

Goszczynski, B. and McGhee, J. D. (2005). Reevaluation of the role of the med-1 and med-2 genes in specifying the Caenorhabditis elegans endoderm. *Genetics* **171**, 545-555.

Herman, M. (2001). C. elegans POP-1/TCF functions in a canonical Wnt pathway that controls cell migration and in a noncanonical Wnt pathway that controls cell polarity. *Development* **128**, 581-590.

Hsu, H. T., Liu, P. C., Ku, S. Y., Jung, K. C., Hong, Y. R., Kao, C. and Wang, C. (2006). Beta-catenin control of T-cell transcription factor 4 (Tcf4) importation from the cytoplasm to the nucleus contributes to Tcf4-mediated transcription in 293 cells. *Biochem. Biophys. Res. Commun.* **343**, 893-898.

Ishitani, T., Ninomiya-Tsuji, J. and Matsumoto, K. (2003). Regulation of lymphoid enhancer factor 1/T-cell factor by mitogen-activated protein kinase-related Nemo-like kinase-dependent phosphorylation in Wnt/beta-catenin signaling. *Mol. Cell. Biol.* **23**, 1379-1389.

Kaletta, T., Schnabel, H. and Schnabel, R. (1997). Binary specification of the embryonic lineage in Caenorhabditis elegans. *Nature* **390**, 294-298.

Kemphues, K. J. and Strome, S. (1997). Fertilization and establishment of polarity in the embryo. In *C. elegans II* (ed. D. L. Riddle, T. Blumenthal, B. J. Meyer and J. R. Priess), pp. 335-360. Plainview, NY: Cold Spring Harbor Laboratory Press.

Kemphues, K. J., Priess, J. R., Morton, D. G. and Cheng, N. S. (1988). Identification of genes required for cytoplasmic localization in early C. elegans embryos. *Cell* **52**, 311-320.

Kidd, A. R., 3rd, Miskowski, J. A., Siegfried, K. R., Sawa, H. and Kimble, J. (2005). A beta-catenin identified by functional rather than sequence criteria and its role in Wnt/MAPK signaling. *Cell* **121**, 761-772.

Korswagen, H. C., Herman, M. A. and Clevers, H. C. (2000). Distinct beta-catenins mediate adhesion and signalling functions in C. elegans. *Nature* **406**, 527-532.

Krieghoff, E., Behrens, J. and Mayr, B. (2006). Nucleo-cytoplasmic distribution of beta-catenin is regulated by retention. *J. Cell Sci.* **119**, 1453-1463.

Lin, R., Thompson, S. and Priess, J. R. (1995). pop-1 encodes an HMG box protein required for the specification of a mesoderm precursor in early C. elegans embryos. *Cell* **83**, 599-609.

Lin, R., Hill, R. J. and Priess, J. R. (1998). POP-1 and anterior-posterior fate decisions in C. elegans embryos. *Cell* **92**, 229-239.

Lo, M. C., Gay, F., Odom, R., Shi, Y. and Lin, R. (2004). Phosphorylation by the beta-catenin/MAPK complex promotes 14-3-3-mediated nuclear export of TCF/POP-1 in signal-responsive cells in C. elegans. *Cell* **117**, 95-106.

Maduro, M. F., Meneghini, M. D., Bowerman, B., Broitman-Maduro, G. and Rothman, J. H. (2001). Restriction of mesendoderm to a single blastomere by the combined action of SKN-1 and a GSK-3beta homolog is mediated by MED-1 and -2 in C. elegans. *Mol. Cell* **7**, 475-485.

Maduro, M. F., Lin, R. and Rothman, J. H. (2002). Dynamics of a developmental switch: recursive intracellular and intranuclear redistribution of Caenorhabditis elegans POP-1 parallels Wnt-inhibited transcriptional repression. *Dev. Biol.* **248**, 128-142.

Maduro, M. F., Hill, R. J., Heid, P. J., Newman-Smith, E. D., Zhu, J., Priess, J. R. and Rothman, J. H. (2005a). Genetic redundancy in endoderm specification within the genus Caenorhabditis. *Dev. Biol.* **284**, 509-522.

Maduro, M. F., Kasmir, J. J., Zhu, J. and Rothman, J. H. (2005b). The Wnt effector POP-1 and the PAL-1/Caudal homeoprotein collaborate with SKN-1 to activate C. elegans endoderm development. *Dev. Biol.* **285**, 510-523.

Mello, C. C., Schubert, C., Draper, B., Zhang, W., Lobel, R. and Priess, J. R. (1996). The PIE-1 protein and germline specification in C. elegans embryos. *Nature* **382**, 710-712.

Meneghini, M. D., Ishitani, T., Carter, J. C., Hisamoto, N., Ninomiya-Tsuji, J., Thorpe, C. J., Hamill, D. R., Matsumoto, K. and Bowerman, B. (1999). MAP kinase and Wnt pathways converge to downregulate an HMG-domain repressor in Caenorhabditis elegans. *Nature* **399**, 793-797.

Miskowski, J., Li, Y. and Kimble, J. (2001). The sys-1 gene and sexual dimorphism during gonadogenesis in Caenorhabditis elegans. *Dev. Biol.* **230**, 61-73.

Mizumoto, K. and Sawa, H. (2007). Cortical beta-catenin and APC regulate asymmetric nuclear beta-catenin localization during asymmetric cell division in C. elegans. *Dev. Cell* **12**, 287-299.

Nakamura, K., Kim, S., Ishidate, T., Bei, Y., Pang, K., Shirayama, M., Trzepacz, C., Brownell, D. R. and Mello, C. C. (2005). Wnt signaling drives WRM-1/beta-catenin asymmetries in early C. elegans embryos. *Genes Dev.* **19**, 1749-1754.

Natarajan, L., Witwer, N. E. and Eisenmann, D. M. (2001). The divergent Caenorhabditis elegans beta-catenin proteins BAR-1, WRM-1 and HMP-2 make distinct protein interactions but retain functional redundancy in vivo. *Genetics* **159**, 159-172.

Park, F. D. and Priess, J. R. (2003). Establishment of POP-1 asymmetry in early C. elegans embryos. *Development* **130**, 3547-3556.

Phillips, B. T., Kidd, A. R., King, R., Hardin, J. and Kimble, J. (2007). Reciprocal asymmetry of SYS-1/beta-catenin and POP-1/TCF controls asymmetric divisions in *Caenorhabditis elegans*. *Proc. Natl. Acad. Sci. USA* **104**, 3231-3236.

Praitis, V., Casey, E., Collar, D. and Austin, J. (2001). Creation of low-copy integrated transgenic lines in Caenorhabditis elegans. *Genetics* **157**, 1217-1226.

Priess, J. R. and Thomson, J. N. (1987). Cellular interactions in early C. elegans embryos. *Cell* **48**, 241-250.

Robertson, S. M., Shetty, P. and Lin, R. (2004). Identification of lineage-specific zygotic transcripts in early Caenorhabditis elegans embryos. *Dev. Biol.* **276**, 493-507.

Rocheleau, C. E., Downs, W. D., Lin, R., Wittmann, C., Bei, Y., Cha, Y. H., Ali, M., Priess, J. R. and Mello, C. C. (1997). Wnt signaling and an APC-related gene specify endoderm in early C. elegans embryos. *Cell* **90**, 707-716.

Rocheleau, C. E., Yasuda, J., Shin, T. H., Lin, R., Sawa, H., Okano, H., Priess, J. R., Davis, R. J. and Mello, C. C. (1999). WRM-1 activates the LIT-1 protein kinase to transduce anterior/posterior polarity signals in C. elegans. *Cell* **97**, 717-726.

Rogers, E., Bishop, J. D., Waddle, J. A., Schumacher, J. M. and Lin, R. (2002). The aurora kinase AIR-2 functions in the release of chromosome cohesion in Caenorhabditis elegans meiosis. *J. Cell Biol.* **157**, 219-229.

Schnabel, H. and Priess, J. R. (1997). Specification of cell fates in the early embryo. In *C. elegans II* (ed. D. L. Riddle, T. Blumenthal, B. J. Meyer and J. R. Priess), pp. 361-382. Plainview, NY: Cold Spring Harbor Laboratory Press.

Schroeder, D. F. and McGhee, J. D. (1998). Anterior-posterior patterning within the Caenorhabditis elegans endoderm. *Development* **125**, 4877-4887.

Shetty, P., Lo, M. C., Robertson, S. M. and Lin, R. (2005). C. elegans TCF protein, POP-1, converts from repressor to activator as a result of Wnt-induced lowering of nuclear levels. *Dev. Biol.* **285**, 584-592.

Shin, T. H., Yasuda, J., Rocheleau, C. E., Lin, R., Soto, M., Bei, Y., Davis, R. J. and Mello, C. C. (1999). MOM-4, a MAP kinase kinase kinase-related protein, activates WRM-1/LIT- 1 kinase to transduce anterior/posterior polarity signals in C. elegans. *Mol. Cell* **4**, 275-280.

Siegfried, K. R. and Kimble, J. (2002). POP-1 controls axis formation during early gonadogenesis in C. elegans. *Development* **129**, 443-453.

Siegfried, K. R., Kidd, A. R., III, Chesney, M. A. and Kimble, J. (2004). The sys-1 and sys-3 genes cooperate with Wnt signaling to establish the proximal-distal axis of the C. elegans gonad. *Genetics* **166**, 171-186.

Sulston, J. E., Schierenberg, E., White, J. G. and Thomson, J. N. (1983). The embryonic cell lineage of the nematode Caenorhabditis elegans. *Dev. Biol.* **100**, 64-119.

Takeshita, H. and Sawa, H. (2005). Asymmetric cortical and nuclear localizations of WRM-1/beta-catenin during asymmetric cell division in C. elegans. *Genes Dev.* **19**, 1743-1748.

Thorpe, C. J. and Moon, R. T. (2004). nemo-like kinase is an essential co-activator of Wnt signaling during early zebrafish development. *Development* **131**, 2899-2909.

Thorpe, C. J., Schlesinger, A., Carter, J. C. and Bowerman, B. (1997). Wnt signaling polarizes an early C. elegans blastomere to distinguish endoderm from mesoderm. *Cell* **90**, 695-705.

Timmons, L. and Fire, A. (1998). Specific interference by ingested dsRNA. *Nature* **395**, 854.

van de Wetering, M., Cavallo, R., Dooijes, D., van Beest, M., van Es, J., Loureiro, J., Ypma, A., Hursh, D., Jones, T., Bejsovec, A. et al. (1997). Armadillo coactivates transcription driven by the product of the Drosophila segment polarity gene dTCF. *Cell* **88**, 789-799.

Yamada, M., Ohnishi, J., Ohkawara, B., Iemura, S., Satoh, K., Hyodo-Miura, J., Kawachi, K., Natsume, T. and Shibuya, H. (2006). NARF, an nemo-like kinase (NLK)-associated ring finger protein regulates the ubiquitylation and degradation of T cell factor/lymphoid enhancer factor (TCF/LEF). *J. Biol. Chem.* **281**, 20749-20760.

Zhu, J., Hill, R. J., Heid, P. J., Fukuyama, M., Sugimoto, A., Priess, J. R. and Rothman, J. H. (1997). end-1 encodes an apparent GATA factor that specifies the endoderm precursor in Caenorhabditis elegans embryos. *Genes Dev.* **11**, 2883-2896.